Developmental Cell, Vol. 9, 403–414, September, 2005, Copyright ©2005 by Elsevier Inc. DOI 10.1016/j.devcel.2005.07.009

The *let-7* MicroRNA Family Members *mir-48*, *mir-84*, and *mir-241* Function Together to Regulate Developmental Timing in *Caenorhabditis elegans*

Allison L. Abbott,[1,4] Ezequiel Alvarez-Saavedra,[2,4] Eric A. Miska,[2,4,5] Nelson C. Lau,[3,6] David P. Bartel,[3] H. Robert Horvitz,[2] and Victor Ambros[1,*]
[1]Department of Genetics
Dartmouth Medical School
Hanover, New Hampshire 03755
[2]Howard Hughes Medical Institute
Department of Biology and
McGovern Institute for Brain Research
Massachusetts Institute of Technology
Cambridge, Massachusetts 02139
[3]Whitehead Institute for Biomedical Research and
Department of Biology
Massachusetts Institute of Technology
9 Cambridge Center
Cambridge, Massachusetts 02142

Summary

The microRNA *let-7* is a critical regulator of developmental timing events at the larval-to-adult transition in *C. elegans*. Recently, microRNAs with sequence similarity to *let-7* have been identified. We find that doubly mutant animals lacking the *let-7* family microRNA genes *mir-48* and *mir-84* exhibit retarded molting behavior and retarded adult gene expression in the hypodermis. Triply mutant animals lacking *mir-48*, *mir-84*, and *mir-241* exhibit repetition of L2-stage events in addition to retarded adult-stage events. *mir-48*, *mir-84*, and *mir-241* function together to control the L2-to-L3 transition, likely by base pairing to complementary sites in the *hbl-1* 3′ UTR and downregulating *hbl-1* activity. Genetic analysis indicates that *mir-48*, *mir-84*, and *mir-241* specify the timing of the L2-to-L3 transition in parallel to the heterochronic genes *lin-28* and *lin-46*. These results indicate that *let-7* family microRNAs function in combination to affect both early and late developmental timing decisions.

Introduction

In *C. elegans*, heterochronic genes control the appropriate temporal execution of stage-specific programs of cell division, cell behavior, and differentiation through the four larval stages, L1–L4 (reviewed in Rougvie, 2001). Mutations in heterochronic genes cause cells in specific lineages to adopt fates normally associated with either earlier or later times in development. Retarded heterochronic mutants reiterate cell fate decisions, and conversely, precocious heterochronic mutants skip cell fate decisions. MicroRNA genes play key roles in this temporal control of larval development (Lee et al., 1993; Reinhart et al., 2000; Rougvie, 2001; Wightman et al., 1993). Progression through the first three larval stages, L1–L3, is controlled by the microRNA *lin-4,* which downregulates the activities of *lin-14* and *lin-28* (Lee et al., 1993; Moss et al., 1997; Wightman et al., 1993). Later in larval development, the *let-7* microRNA controls the L4-to-adult transition (Reinhart et al., 2000) through the downregulation of *hbl-1* (Abrahante et al., 2003; Lin et al., 2003), *lin-41* (Slack et al., 2000; Vella et al., 2004), and *daf-12* (Grosshans et al., 2005). The repression of *hbl-1* and *lin-41* allows for the activation of the adult-specific transcription factor *lin-29*. *lin-29* mutants, which repeat the L4-stage program indefinitely, display a stronger heterochronic phenotype than *let-7* mutants, which repeat the L4-stage program only once. This suggests that other genes in addition to *let-7* act upstream of *lin-29* in the heterochronic gene pathway to specify the appropriate execution of the adult-stage program. Overexpression of *mir-84* results in heterochronic defects (Johnson et al., 2005), further suggesting a role for additional microRNAs in the developmental timing pathway.

Recent cloning and computational efforts have expanded the number of known and predicted microRNAs (Bartel, 2004; Berezikov et al., 2005) to include approximately 100 genes in *C. elegans* (Ambros et al., 2003; Grad et al., 2003; Lau et al., 2001; Lee and Ambros, 2001; Lim et al., 2003; Ohler et al., 2004). As exemplified by *let-7*, microRNA genes can be extensively conserved across diverse animal taxa, including worms, flies, and humans (Pasquinelli et al., 2000). Many additional microRNAs can be grouped into "families" based primarily on sequence similarity at the 5′ portion of the microRNAs (Ambros et al., 2003; Grad et al., 2003; Lewis et al., 2003; Lim et al., 2003). Three *C. elegans* genes, *mir-48*, *mir-84*, and *mir-241*, that share complete sequence identity with *let-7* for eight consecutive nucleotides at their 5′ ends were identified (Lau et al., 2001; Lim et al., 2003).

To examine the functions of the *let-7* family members *mir-48*, *mir-84*, and *mir-241*, we isolated mutants by screening a library of mutagenized worms for deletion mutations. We show that *mir-48*, *mir-84*, and *mir-241* function together to control developmental timing at the L2-to-L3 transition. Although *hbl-1* activity was previously shown to function primarily downstream of *let-7* in the L4-to-adult transition, we provide evidence that *hbl-1* also functions in the L2-to-L3 transition and that *hbl-1*, but not *lin-28*, is a likely downstream target of *mir-48*, *mir-84*, and *mir-241* activity.

Results

Expression of *mir-48*, *mir-84*, and *mir-241* and Isolation of Deletion Mutations

The "*let-7* family" is comprised of *let-7* and three other *C. elegans* microRNA genes, *mir-48*, *mir-84*, and *mir-*

*Correspondence: victor.r.ambros@dartmouth.edu
[4]These authors contributed equally to this work.
[5]Present address: Wellcome Trust/Cancer Research UK Gurdon Institute, University of Cambridge, Tennis Court Road, Cambridge, CB2 1QN, United Kingdom.
[6]Present address: Department of Molecular Biology, Massachusetts General Hospital, 55 Fruit Street, Boston, Massachusetts 02114.

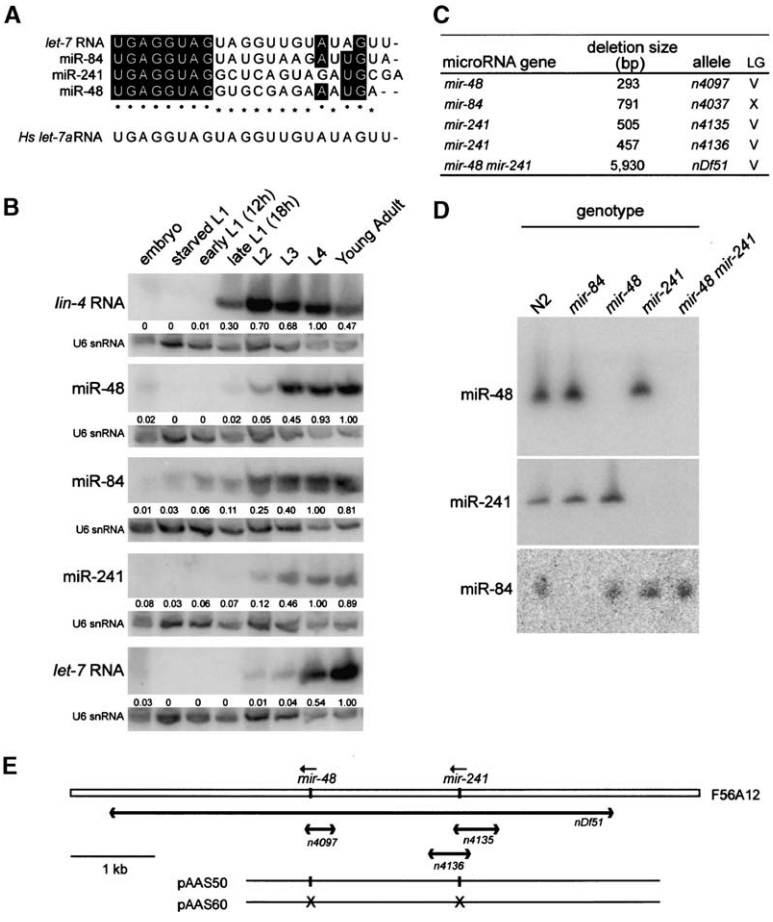

Figure 1. Isolation of Deletion Alleles of the *let-7* Family MicroRNA Genes *mir-48*, *mir-84*, and *mir-241*

(A) Alignment of mature ~22 nt microRNA sequences of the four *C. elegans let-7* family members and the human *let-7* RNA (*hs let-7*). Shaded boxes and asterisks indicate bases conserved in two or three worm family members, respectively.

(B) Temporal expression patterns of *let-7* family microRNA genes, *mir-48*, *mir-84*, *mir-241*, and *let-7*. Northern blot analysis of RNA isolated from populations of staged worms. As a control for staging of the worms during early larval development, *lin-4* expression is observed during the late L1 stage. Northern blots indicate that miR-241, miR-48, and miR-84 reached half-maximal expression at about the L3 stage, while *let-7* RNA reached half-maximal expression at about the L4 stage. Each blot was stripped and probed for U6 snRNA expression to standardize loading of RNA samples. The numbers underneath each band indicate the signal of the corresponding microRNA normalized to that of U6 snRNA presented relative to maximal expression for each microRNA.

(C) List of deletion mutations isolated in the *mir-48*, *mir-84*, and *mir-241* genes.

(D) Northern blot analysis of RNA isolated from wild-type or mutant animals and hybridized with probes to the mature ~22 nt microRNA sequences for miR-48, miR-241, and miR-84. The deletion mutations result in the loss of the corresponding ~22 nt mature microRNA for miR-48, miR-241, and miR-84.

(E) The *mir-48* and *mir-241* locus on chromosome V. The mature microRNA sequences are located within a 1.8 kb genomic region on cosmid F56A12. Deletions at this locus are shown below. The deficiency *nDf51* removes both the *mir-48* and *mir-241* mature microRNA sequences. For rescue experiments, we injected the plasmid pAAS50, which contains a 5073 bp fragment of genomic DNA encompassing both the *mir-48* and *mir-241* mature microRNA sequences. For control experiments, we injected the plasmid pAAS60, which was generated from pAAS50 but lacked the sequences corresponding to the *mir-48* and *mir-241* mature microRNA sequences.

241 (Lau et al., 2001; Lim et al., 2003), based on the complete conservation of eight nucleotides at their 5′ ends (Figure 1A). To compare temporal expression profiles of the *let-7* family microRNAs, Northern blot analysis was performed on RNA isolated from populations of staged worms (Figure 1B). Although all of the *let-7* family members reached half-maximal expression after *lin-4* RNA, their temporal expression profiles during larval development differed from each other: when normalized to U6 expression, miR-241, miR-48, and miR-84 reached half-maximal expression at about the L3 stage, while *let-7* RNA reached half-maximal expression at about the L4 stage (Figure 1B). Previous studies did not detect the four *let-7* family members until the L3 stage (Lau et al., 2001; Lim et al., 2003; Reinhart et al., 2000), but we were able to detect earlier expression of all four microRNAs by enhancing the sensitivity of detection (see Experimental Procedures).

To examine the functions of *mir-48*, *mir-84*, and *mir-241*, we isolated worms with deletion mutations in the corresponding genomic loci. These deletions remove the genomic sequence corresponding to the ~22 nt mature microRNA along with flanking regions (Figure 1C). Absence of the ~22 nt mature microRNA in mutant worms was confirmed by Northern blot (Figure 1D). Deletions in single *let-7* family member genes did not appreciably affect the expression of the remaining family members. For example, a deletion upstream of *mir-48* that removes *mir-241* affected the expression of neither *mir-48* nor *mir-84*, as determined by Northern blot analysis of RNA isolated from a population of mixed-stage worms (Figure 1D). Because *mir-48* and *mir-241* are located within a 2 kb region in the *C. elegans* genome, we also isolated worms with a deletion, *nDf51*, that removes both of these microRNA genes (Figure 1E).

mir-48 Single Mutants and *mir-48; mir-84* Double Mutants Undergo an Extra Adult Molt

Singly mutant worms with deletions in *mir-48*, *mir-84*, or *mir-241* displayed an essentially normal phenotype when cultured under standard conditions at 20°C (Table 1). However, at 15°C, adult-stage *mir-48* mutants exhibited a weak retarded defect: 69% of young adults inappropriately entered lethargus and executed a partially complete supernumerary molt and sometimes became

Table 1. Phenotypic Consequences of and Genetic Interactions among *mir-48*, *mir-84*, and *mir-241* Mutations

		Average Number of Seam Cells				Percentage of Worms with Alae Formation					
							L4 Molt[a]				
Strain	Genotype	L2	L3	L4[a]	L4 Molt[a]	Early L4[a]	No Alae	Gapped	Complete	Percent Lethality at L4 Molt	Percentage of Adult-Stage Lethargus
N2	wild-type	11 (20)	11 (20)	11 (20)	11 (21)	0	0	0	100	0 (104)	0 (104)
MT13650	*mir-48(n4097)*	—[b]	—	—	11 (22)	0	0	5	95	0 (39)	4 (135)
MT13650	*mir-48(n4097)* @ 15°C	—	—	—	11 (20)	0	0	5	95	0 (66)	69 (185)
MT13651	*mir-84(n4037)*	—	—	—	12 (20)	0	0	0	100	0 (71)	0 (71)
MT13896	*mir-241(n4135)*	—	—	—	11 (13)	0	0	0	100	0 (81)	0 (81)
MT13897	*mir-241(n4136)*	—	—	—	11 (22)	0	0	0	100	0 (35)	0 (35)
MT14118	*mir-241(n4136); mir-84(n4037)*	—	—	—	11 (20)	0	0	5	95	0 (110)	0 (110)
MT13652	*mir-48(n4097); mir-84(n4037)*	—	—	—	11 (20)	0	0	0	100	0 (72)	79 (72)
MT13669	*mir-48 mir-241(nDf51)*	11 (24)	16 (24)[c]	16 (29)[c]	16 (27)[c]	0	8	92	0	37 (81)	36 (81)
VT1066	*mir-48 mir-241(nDf51); mir-84(n4037)*	11 (23)	19 (31)[c]	20 (20)[c]	20 (20)[c]	0	47	47	6	79 (80)	16 (80)
MT14749	*mir-48 mir-241(nDf51); nEx1185*[d]	—	—	—	12 (32)[e,f]	—	0	13	87	—	—
MT14778	*mir-48 mir-241(nDf51); nEx1192*[g]	—	—	—	17 (18)[e,h]	—	0	80	20	—	—
VT517	*lin-28(n719)*	—	6 (21)[c]	6 (18)[c]	—	100	—	—	—	0 (108)	—
VT1103	*lin-28(n719); mir-48 mir-241(nDf51); mir-84(n4037)*	—	7 (25)[c]	6 (19)[c]	—	100	—	—	—	1 (100)	—
VT786	*lin-46(ma164)*	—	—	—	12 (26)	—	0	12	88	1 (110)	—
VT1145	*lin-46(ma164); mir-48 mir-241(nDf51); mir-84(n4037)*	—	21 (17)[c]	39 (17)[c]	44 (20)[c]	0	100	0	0	0 (106)	—
VT937	*lin-28(n719); lin-46(ma164)*	—	—	—	11 (22)	—	0	0	100	0 (89)	—
VT1102	*lin-28(n719); lin-46(ma164) mir-48 mir-241(nDf51); mir-84(n4037)*	11 (21)	22 (20)[c]	38 (21)[c]	39 (20)[c]	0	100	0	0	22 (27)	—
RG559	*hbl-1(ve18)*	—	11 (21)	13 (24)	14 (18)	25	0	9	91	9 (34)	—
VT1146	*hbl-1(ve18) mir-84(n4037); mir-48 mir-241(nDf51)*	—	11 (17)	13 (22)	13 (23)	0	0	33	67	9 (57)	—
CT8	*lin-41(ma104)*	—	—	11 (27)	11 (25)	19	4	0	96	7 (90)	—
VT1143	*lin-41(ma104); mir-48 mir-241(nDf51); mir-84(n4037)*	11 (20)	17 (16)[c]	17 (20)[c]	18 (20)[c]	0	0	85	15	3 (97)	—

[a] Worms scored at the L4 and L4 molt stages for both seam cells and alae formation. Number of worms (n) scored for each group is indicated in parentheses.
[b] —, did not score.
[c] $p < 0.01$ (comparison with N2).
[d] Extrachromosomal array from injecting 100 ng/μl pAAS50 and 20 ng/μl pTG96 (*sur-5::GFP*). pAAS50 is a pCR-II TOPO plasmid containing a 5073 bp fragment that contains *mir-48* and *mir-241*.
[e] Worms scored for number of seam cells at the L4 or L4 molt stages. Three lines scored independently for rescue experiments. Data from representative lines are shown.
[f] $p < 0.001$ (comparison with *nDf51*).
[g] Extrachromosomal array from injecting 100 ng/μl pAAS60 and 20 ng/μl pTG96 (*sur-5::GFP*). pAAS60 is the same as pAAS50, except that the sequences corresponding to the mature microRNAs *mir-48* and *mir-241* have been deleted.
[h] $p > 0.05$ (comparison with *nDf51*).

trapped in the unshed cuticle (Table 1). This phenotype was also observed at a low penetrance (4%, Table 1) when *mir-48* animals were cultured at 20°C. *mir-84* and *mir-241* single mutants had no observable abnormal phenotype at 15°C (data not shown). Thus, like *let-7* mutants, *mir-48* animals execute a supernumerary molt. However, the characteristics of the extra molt differ: *let-7* animals fail to execute the L4-to-adult transition and display an extra larval molt, whereas *mir-48* mutants execute the L4-to-adult transition apparently normally and then undergo an extra adult molt.

To test whether *mir-48*, *mir-84*, and *mir-241* function redundantly, double and triple mutants were generated. *mir-84; mir-241* animals displayed no detectable abnor-

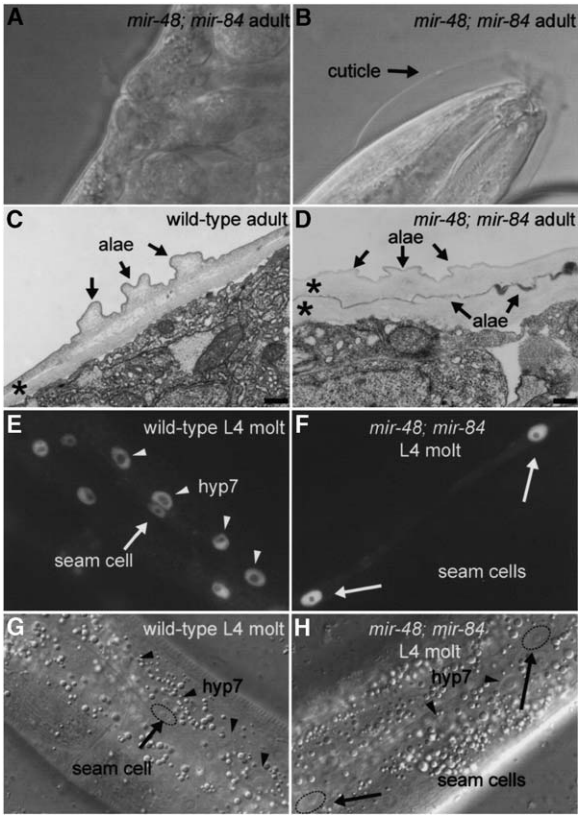

Figure 2. *mir-48; mir-84* Double Mutants Display Supernumerary Molting Behavior in Adult Worms

(A and B) Nomarski DIC images of a *mir-48; mir-84* animal with a (A) fully formed vulva and with embryos visible inside of the worm to show that the worm is in the adult stage and (B) unshed cuticle surrounding the anterior region of the worm.

(C and D) Electron micrographs of adult-stage cuticle in a (C) wild-type animal and a (D) *mir-48; mir-84* adult. Asterisks indicate cuticles. The scale bar is 300 nm. (C) Normal single cuticle with alae in a wild-type adult. (D) Two cuticles, both with alae structures (arrows), are visible in a *mir-48; mir-84* adult.

(E and F) Fluorescence micrographs of a (E) wild-type and a (F) *mir-48; mir-84* worm at the L4 molt stage that carry the *col-19::gfp* transgene *mals105*. (E) Fluorescence micrograph of a wild-type L4 molt-stage worm. Expression of *col-19::gfp* is observed in nuclei of the hyp7 syncytium (arrowheads) and hypodermal seam cells (arrows) in a wild-type L4 molt-stage-worm. (F) Expression of *col-19::gfp* is observed in hypodermal seam cells (arrows) in a *mir-48; mir-84* L4 molt-stage worm. *col-19::gfp* expression is reduced or absent in hyp7.

(G and H) Nomarski DIC images of the hypodermis of the animals in (E) and (F), respectively, showing seam cell (arrows) and hyp7 (arrowheads) nuclei.

malities (Table 1). *mir-48; mir-84* adult-stage animals exhibited a strongly penetrant extra molting phenotype at 20°C (Figures 2A and 2B; Table 1), similar to that of *mir-48* mutant animals at 15°C. By electron microscopy, two cuticles, both with adult lateral alae, were apparent on *mir-48; mir-84* adults (Figure 2D), in contrast to the single cuticle on wild-type adults (Figure 2C). At the L4 molt, *mir-48; mir-84* animals displayed no abnormal phenotype in the lateral hypodermal seam cells; worms had the normal number of seam cells generated from the V lineage, complete alae formation, and normal expression of the adult stage-specific transgene *col-19::gfp* (Abrahante et al., 1998; Liu et al., 1995). In contrast, in the main body hypodermal syncytial cell, hyp7, *col-19::gfp* expression was reduced or absent in *mir-48; mir-84* worms at the L4 molt (Figure 2F). Thus, in *mir-48; mir-84* double mutants at the L4 molt, hyp7 displayed larval characteristics and likely failed to make the larval-to-adult transition appropriately. The supernumerary molting phenotype of *mir-48; mir-84* animals may be a consequence of the retarded state of hyp7. In contrast, the hypodermal seam cells in *mir-48; mir-84* double mutants at the L4 molt primarily displayed adult characteristics: seam cells stopped dividing, formed alae, and expressed *col-19::gfp*. This is a weaker heterochronic phenotype than that of *let-7*(lf) worms. Whereas *mir-48; mir-84* worms exhibited a larval-to-adult delay only in hyp7, *let-7*(lf) worms exhibit a larval-to-adult delay in both hyp7 and in the seam cells.

Seam Cells of *mir-48 mir-241* Double Mutants and *mir-48 mir-241; mir-84* Triple Mutants Repeat the L2-Stage Developmental Program

mir-48 mir-241 double mutants and *mir-48 mir-241; mir-84* triple mutants displayed a retarded cell lineage phenotype in the lateral hypodermis. Extra seam cells were observed at the L3 and L4 stages (Table 1, Figure 3C) compared to wild-type worms (Table 1, Figure 3A). In the L2-stage of wild-type worms, five of the six V lineage seam cells on each side of the animal execute a "proliferative" program with two rounds of cell division, which results in an increase in the number of seam cells from six in the L1 stage to 11 in the L2 stage. In the L3 and L4 stages, a single stem cell-like division occurs, with only the posterior daughter retaining seam cell identity. Therefore, the number of V lineage seam cells on each side of wild-type animals remains constant at 11 after the L2 stage. However, in *mir-48 mir-241* and in *mir-48 mir-241; mir-84* L3 larvae, the average number of V lineage seam cells was 16 (range = 11–18) and 19 (range = 14–23), respectively. No further increase in the number of seam cells was detected in L4 larvae. In addition, *mir-48 mir-241; mir-84* triple mutants failed to generate complete alae at the L4 molt (Table 1). The retarded seam cell and alae phenotypes were not observed in mutants transformed with a 5 kb genomic fragment containing the *mir-48* and *mir-241* loci (Table 1, Figure 1E), indicating that the defect was caused by mutations within the 5 kb region corresponding to the transgene. Further, when the sequences for *mir-48* and *mir-241* mature ~22 nt microRNAs were deleted from this genomic fragment, no rescue was observed, indicating that the phenotype was caused specifically by loss of the microRNA sequences (Table 1, Figure 1E).

We hypothesized that the extra seam cells observed in *mir-48 mir-241* and *mir-48 mir-241; mir-84* mutants arose from inappropriate repetition of the L2-stage seam cell proliferative program during the L3 stage. To investigate this possibility, we observed seam cell division patterns in individual *mir-48 mir-241* and *mir-48 mir-241; mir-84* mutant worms from the late-L2 stage through the L3 stage. In all animals examined, two rounds of cell division were observed in V lineage seam

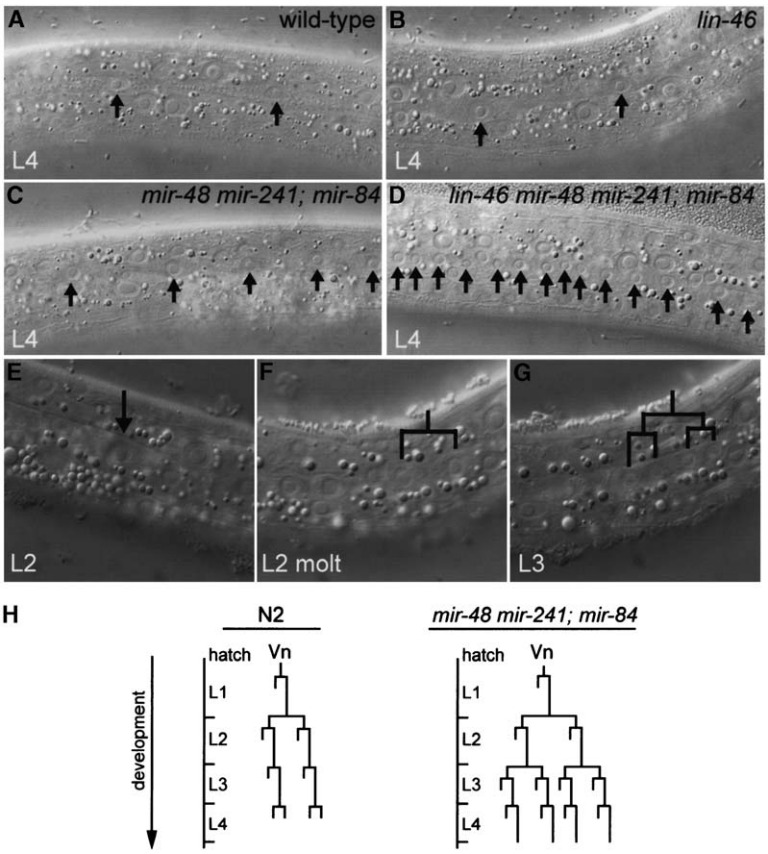

Figure 3. Extra Seam Cells Generated as a Consequence of Reiteration of the L2-Stage Developmental Program in Animals Lacking *mir-48*, *mir-84*, and *mir-241* MicroRNA Activity

Nomarski DIC images of the hypodermis.

(A and B) Arrows indicate seam cells. Normal seam cell number is observed in a (A) wild-type and (B) *lin-46* mutant animal at the L4 stage.

(C) Extra seam cells in a *mir-48 mir-241; mir-84* triple mutant at the L4 stage.

(D) Enhanced extra-seam-cell phenotype of a *lin-46 mir-48 mir-241; mir-84* mutant animal at the L4 stage.

(E–G) Sequential Nomarski DIC images of a *mir-48 mir-241; mir-84* mutant animal (E) during the late L2 stage, (F) during the L2 molt, and (G) during the early L3 stage. The same V seam cell lineage in a single animal is shown in all three images. (E) A single seam cell prior to cell division (arrow). (F) The seam cell in (E) divided during the L2 molt, resulting in two daughters. (G) Each of the daughters from (F) executed another round of cell divisions, resulting in four daughter nuclei in the early-L3 stage. The posterior daughter of each pair of daughter nuclei retains the seam cell identity, and the anterior daughter fuses with the hyp7 syncytium (Sulston and Horvitz, 1977).

(H) Diagram of Vn (V1–V4, V6) lineage of a normal N2 wild-type animal (adapted from Sulston and Horvitz, 1977) and a *mir-48 mir-241; mir-84* triple mutant animal. Reiteration of the L2-stage proliferative program is observed in V lineage seam cells of *mir-48 mir-241; mir-84* triple mutants.

cells during the L3 stage (Figures 3E–3G). The number of seam cells observed by lineage analysis to undergo an extra round of cell division varied among individual worms (range = 3–10 of 11 V lineage seam cells, n = 6). This variability was consistent with the range of seam cell numbers counted in L3-stage worms (see above). These data demonstrate that *mir-48 mir-241* doubly mutant and *mir-48 mir-241; mir-84* triply mutant worms repeat the L2-stage developmental program in the lateral hypodermal seam cells during the L3 stage and indicate that *mir-48*, *mir-84*, and *mir-241* act redundantly to specify the appropriate timing of stage-specific seam cell behavior.

Do *mir-48*, *mir-84*, and *mir-241* Act through *lin-28* to Control the L2-to-L3 Transition?

The heterochronic gene *lin-28* is a key regulator of the timing of L2-stage events in the hypodermis. In *lin-28*(lf) mutants, the L2-stage seam cell proliferative program is skipped (Ambros and Horvitz, 1984). In contrast, seam cells of *mir-48 mir-241; mir-84* animals repeat the L2-stage program. Thus, *lin-28* and *mir-48 mir-241; mir-84* have opposing activities. To determine the relationship between *mir-48*, *mir-84*, *mir-241*, and *lin-28*, we performed genetic epistasis analysis. We found that *lin-28*(lf); *mir-48 mir-241; mir-84* worms displayed a precocious phenotype like that of *lin-28*(lf), including reduced numbers of seam cells and precocious adult alae during the L4 stage (Table 1). Thus, the *lin-28* precocious phenotype in the hypodermis was epistatic to the *mir-48 mir-241; mir-84* retarded phenotype. Because the *lin-28* 3′ UTR contains a putative *let-7* binding site (Reinhart et al., 2000), *mir-48*, *mir-84*, and *mir-241* could act to directly repress the activity of *lin-28*; alternatively, *mir-48*, *mir-84*, and *mir-241* could act in an independent parallel pathway to control the L2-to-L3 transition.

If *lin-28* is a target of *mir-48*, *mir-84*, and *mir-241*, then the level of LIN-28 protein should be elevated in *mir-48 mir-241; mir-84* triple mutants. To test this, we used a *lin-28::gfp::lin-28* fusion construct to monitor the LIN-28 protein level (Moss et al., 1997). In wild-type worms, *lin-28::gfp::lin-28* is expressed most abundantly in the L1 stage, is downregulated beginning at the L2 stage, and is essentially absent by the L3 and L4 stages (Moss et al., 1997). We observed no abnormalities in the downregulation of *lin-28::gfp::lin-28* expression in *mir-48 mir-241; mir-84* triple mutants (Figure S1; see the Supplemental Data available with this article online). In contrast, *lin-28::gfp::lin-28* expression remained elevated in *lin-4*(lf) worms (Figure S1, Moss et al., 1997). Western blot analysis also indicated little, if any, increase in LIN-28 protein levels in the absence of *mir-48*, *mir-84*, and *mir-241* (data not shown). The apparently normal downregulation of LIN-28 in the absence of *mir-48*, *mir-84*, and *mir-241* suggests that *lin-28* is not a direct target of these microRNAs.

If *lin-28* is not a target of the *mir-48*, *mir-84*, and *mir-241* microRNAs, but rather acts in a parallel pathway, then what accounts for the epistasis of *lin-28* over *mir-48*, *mir-84*, and *mir-241*? This epistasis could be explained by the function of *lin-46*, a downstream effector of *lin-28*. *lin-46* acts downstream of *lin-28* to specify L3-specific cell fates, and mutations in this gene completely suppress the precocious phenotype of *lin-28*(lf) mutants (Pepper et al., 2004). If *mir-48*, *mir-84*, and *mir-241* function in a pathway parallel to both *lin-28* and *lin-46* to control the L2-to-L3 transition, then retarded development like that in *mir-48 mir-241; mir-84* triple mutants is predicted for *lin-28*(lf); *lin-46*(lf) *mir-48 mir-241; mir-84* worms. Indeed, despite the complete absence of *lin-28* activity, *lin-28*(lf); *lin-46*(lf) *mir-48 mir-241; mir-84* quintuply mutant worms displayed a strong retarded phenotype with extra seam cells and retarded adult alae formation (Table 1). This observation provides additional evidence that the L2 reiteration phenotype is not caused primarily by elevated levels of *lin-28* activity. Therefore, we propose that *mir-48*, *mir-84*, and *mir-241* function in a pathway parallel to *lin-28* and *lin-46*, and that these pathways converge on a shared downstream effector to control the L2-to-L3 transition.

Interestingly, the *lin-28*(lf); *lin-46*(lf) *mir-48 mir-241; mir-84* quintuply mutant animals displayed a stronger retarded phenotype than that of *mir-48 mir-241; mir-84* triple mutants. Whereas *mir-48 mir-241; mir-84* worms reiterated the L2-stage program only once in the L3 stage, *lin-28*(lf); *lin-46*(lf) *mir-48 mir-241; mir-84* worms had a greater number of seam cells in L4-stage worms, consistent with an additional execution of the L2-stage developmental program in the L4 stage (Table 1). Moreover, vulva formation was retarded in *lin-28*(lf); *lin-46*(lf) *mir-48 mir-241; mir-84* worms, while vulva formation in *mir-48 mir-241; mir-84* triple mutants occurred with no obvious timing defects. The retarded phenotype observed in *lin-28*(lf); *lin-46*(lf) *mir-48 mir-241; mir-84* worms was independent of *lin-28* activity, in that the same phenotype was observed in *lin-46*(lf) *mir-48 mir-241; mir-84* worms (Table 1, Figure 3D). *lin-46*(lf) single mutants display an L2 reiteration phenotype at 15°C, but not, however, at 20°C (Pepper et al., 2004) (Figure 3C). Our data indicate that *lin-46* likely acts in parallel with *mir-48*, *mir-84*, and *mir-241* to specify L3-stage events.

Depletion of *hbl-1* Activity, but Not *lin-41* Activity, Suppresses *mir-48 mir-241; mir-84* Defects at the L2-to-L3 Transition

One candidate downstream effector of *mir-48*, *mir-84*, and *mir-241* activities is the *C. elegans hunchback* homolog *hbl-1* (Fay et al., 1999). *hbl-1* regulates developmental timing and also contains eight *let-7* complementary sites in its 3′ UTR (Abrahante et al., 2003; Lin et al., 2003). If the L2 reiteration phenotype of *mir-48 mir-241; mir-84* animals is caused by failure to repress *hbl-1*, then it is expected that a decrease in *hbl-1* activity, either genetically with the partial loss-of-function *hbl-1* allele, *ve18* (Abrahante et al., 2003; Lin et al., 2003), or by RNAi, should suppress this phenotype. *mir-48 mir-241; hbl-1(ve18) mir-84* mutant worms did not display extra seam cells at the L3 stage (Table 1), indicating that *hbl-1(ve18)* suppressed the L2 reiteration phenotype. The retarded alae phenotype caused by the loss of *mir-48*, *mir-84*, and *mir-241* was also suppressed; at the L4 molt, 85% of *mir-48 mir-241; hbl-1(ve18) mir-84* quadruply mutant worms exhibited complete alae formation, compared to only 6% of *mir-48 mir-241; mir-84* triple mutants (Table 1). Similar results were obtained when *hbl-1* activity was depleted by RNAi in *mir-48 mir-241; mir-84* animals. *hbl-1*(RNAi) administered postembryonically resulted in strong suppression of the L2 reiteration phenotype of L3-stage *mir-48 mir-241; mir-84* worms and suppression of the retarded alae phenotype at the L4 molt (Table 2). *hbl-1*(RNAi) also suppressed the enhanced L2 reiteration phenotype of *lin-46*(lf) *mir-48 mir-241; mir-84* animals (Table 2), suggesting that both the *lin-46* and the *mir-48*, *mir-84*, and *mir-241* pathways converge on *hbl-1* to control the L2-to-L3 transition.

Because *lin-41* acts redundantly with *hbl-1* to regulate the L4-to-adult transition (Abrahante et al., 2003; Lin et al., 2003), we tested whether *lin-41* might also act with *hbl-1* to regulate the L2-to-L3 transition. Unlike reduction of *hbl-1* activity, reduction of *lin-41* activity had little effect on the L2 reiteration phenotype (Tables 1 and 2), but did partially suppress the retarded alae phenotype (Table 2). These data indicate that *mir-48*, *mir-84*, and *mir-241* control the L2-to-L3 transition by repressing *hbl-1* and not by repressing *lin-41*.

mir-48, *mir-84*, and *mir-241* Are Necessary for Temporal Downregulation of *hbl-1* Expression

If *mir-48*, *mir-84*, and *mir-241* regulate *hbl-1* expression during wild-type development, then *mir-48 mir-241; mir-84* triple mutants should exhibit an elevated level of HBL-1 protein. *hbl-1* is expressed in the hypodermis during embryogenesis, and this expression decreases during early larval development, becoming undetectable by the L3 stage (Abrahante et al., 2003; Fay et al., 1999; Lin et al., 2003). The repression of *hbl-1* in the hypodermal syncytium hyp7 during early larval development requires the *hbl-1* 3′ UTR (Abrahante et al., 2003; Lin et al., 2003). To test whether *hbl-1* activity is upregulated in *mir-48 mir-241; mir-84* triple mutants, we used an *hbl-1::gfp::hbl-1* fusion construct as a reporter for the level of HBL-1 protein (Fay et al., 1999). In 80% of *mir-48 mir-241; mir-84* triple mutants at the L3 stage, *hbl-1::gfp::hbl-1* expression was detected in hyp7 (Figure 4D). In contrast, *hbl-1::gfp::hbl-1* expression was detected in hyp7 in only 11% of wild-type worms at the L3 stage (Figure 4C). Our data are consistent with a model that *mir-48*, *mir-84*, and *mir-241* act together to regulate the level of HBL-1 protein in hyp7. However, because single and double mutants that do not display the L2 reiteration phenotype were not examined for elevated *hbl-1::gfp::hbl-1* activity, it remains possible that the individual family members, *mir-48*, *mir-84*, and *mir-241*, differ in their capacity to repress *hbl-1* activity.

Discussion

Functional Cooperation among MicroRNA Family Members

Our data demonstrate that the *let-7* family microRNA genes *mir-48*, *mir-84*, and *mir-241* function together to

Table 2. *hb1-1* Depletion by RNAi Suppresses the Phenotype of Extra Seam Cells and Retarded Alae of a *mir-48 mir-241; mir-84* Triple Mutant and of a *lin-46 mir-48 mir-241; mir-84* Mutant

Strain	Genotype	dsRNA Construct	Number of Seam Cells (n)		Percentage of Worms with Precocious Alae during L4				Percentage of Worms with Alae at L4 Molt/Young Adult			
			L3	L4	No Alae	Gapped	Complete	n	No Alae	Gapped	Complete	n
N2	wild-type	control	11 (15)	11 (20)	100	0	0	20	0	0	100	26
		hbl-1	9 (33)	10 (33)	0	24	76	33	0	14	86	7
		lin-41	11 (16)	11 (40)	60	40	0	40	0	29	71	24
		hbl-1 and *lin-41*	10 (27)	11 (35)	3	57	40	35	0	46	54	13
VT1066	*mir-48 mir-241; mir-84*	control	17 (21)	19 (23)	100	0	0	23	43	54	4	28
		hbl-1	9 (33)	14 (48)	89	11	0	36	0	32	68	25
		lin-41	16 (20)	17 (32)	93	7	0	29	0	47	53	30
		hbl-1 and *lin-41*	10 (20)	11 (30)	0	60	40	25	0	29	71	21
VT786	*lin-46*	control	12 (9)	12 (20)	100	0	0	20	0	19	81	26
		hbl-1	9 (6)	10 (20)	0	20	80	20	0	0	100	15
		lin-41	12 (1)	12 (21)	81	19	0	21	0	12	88	17
		hbl-1 and *lin-41*	8 (3)	10 (20)	11	37	53	19	0	8	92	24
VT1145	*lin-46 mir-48 mir-241; mir-84*	control	22 (17)	40 (20)	100	0	0	20	100	0	0	18
		hbl-1	10 (24)	14 (36)	100	0	0	36	0	80	20	20
		lin-41	22 (20)	40 (31)	100	0	0	31	100	0	0	36
		hbl-1 and *lin-41*	11 (22)	11 (36)	0	50	50	36	0	29	71	17

control developmental timing in *C. elegans*. Synthetic heterochronic phenotypes were observed in double and triple mutants, indicating functional cooperation or redundancy among these *let-7* family microRNAs. *mir-48* single mutants displayed a supernumerary adult-stage lethargus. The penetrance of this phenotype was greatly enhanced in *mir-48; mir-84* double mutants. *mir-48 mir-241* double mutants also displayed extra seam cell divisions during the L3 stage, the formation of incomplete adult-stage alae, and lethality associated with vulva bursting at the L4-to-adult transition. All of these retarded heterochronic defects occurred with higher frequency in triply mutant worms that lack *mir-48*, *mir-84*, and *mir-241*.

The *C. elegans* genome encodes at least 19 microRNA gene families containing from 2 to 8 members with significant sequence conservation within the ~22 nt microRNA sequence (Ambros et al., 2003; Grad et al., 2003; Lim et al., 2003). Sequence conservation among family members is strongest near the 5′ end of the microRNA in the region known as the "seed," which has been proposed to reflect a potential for family members to direct the repression of shared target genes (Bartel, 2004; Brennecke et al., 2005; Doench and Sharp, 2004; Kloosterman et al., 2004; Lai, 2002; Lewis et al., 2003, 2005; Lim et al., 2005; Mallory et al., 2004; Stark et al., 2003). Because *mir-48*, *mir-84*, and *mir-241* display complete sequence conservation in the seed region at the 5′ end, it is possible that they could repress a common set of targets and hence could be functionally equivalent. Our findings suggest that *let-7*, *mir-48*, *mir-84*, and *mir-241* may all act to repress a shared target, *hbl-1* (see below). *let-60 RAS* also has been proposed to be a target of *mir-84* based on overexpression experiments (Johnson et al., 2005). Elevated levels of *let-60 RAS* expression lead to a multivulva phenotype (Beitel et al., 1990; Han and Sternberg, 1990); however, we did not observe a multivulva phenotype in *mir-84* single mutants nor in *mir-48 mir-241; mir-84* triple mutants.

Our results leave open the possibility that *mir-48*, *mir-84*, and *mir-241* are not functionally equivalent in all respects. Sequence differences in the 3′ end of the *let-7* family microRNAs may direct the repression of some distinct sets of targets, the repression of which could function coordinately to regulate developmental timing. Target sites that lack strong complementarity at the microRNA 5′ end can direct repression if there is extensive compensatory pairing at the 3′ end, thus allowing for distinct activities of microRNA family members (Brennecke et al., 2005; Doench and Sharp, 2004). Indeed, *let-7* complementary sites in the *lin-41* mRNA have extensive complementarity to the *let-7* 3′ region, along with imperfect pairing to the *let-7* 5′ seed region (Slack et al., 2000). The specificity imparted by compensatory 3′ pairing may function to enable repression of *lin-41* by *let-7* and not allow for the repression of *lin-41* by *mir-48*, *mir-84*, or *mir-241* (Brennecke et al., 2005; Lewis et al., 2005). Similarly, extensive 3′ pairing to one of the other three *let-7* family members might compensate for a lack of strong 5′ pairing and therefore could restrict the repression of specific targets to individual *let-7* family members.

hbl-1 Is Likely a Direct Target of the *let-7* Family of MicroRNAs

Our findings suggest that the four *let-7* family microRNAs may all act to repress *hbl-1*. Reduction of *hbl-1* activity can suppress the heterochronic defects observed in both *mir-48 mir-241; mir-84* (this study) and *let-7* (Abrahante et al., 2003; Lin et al., 2003) mutant

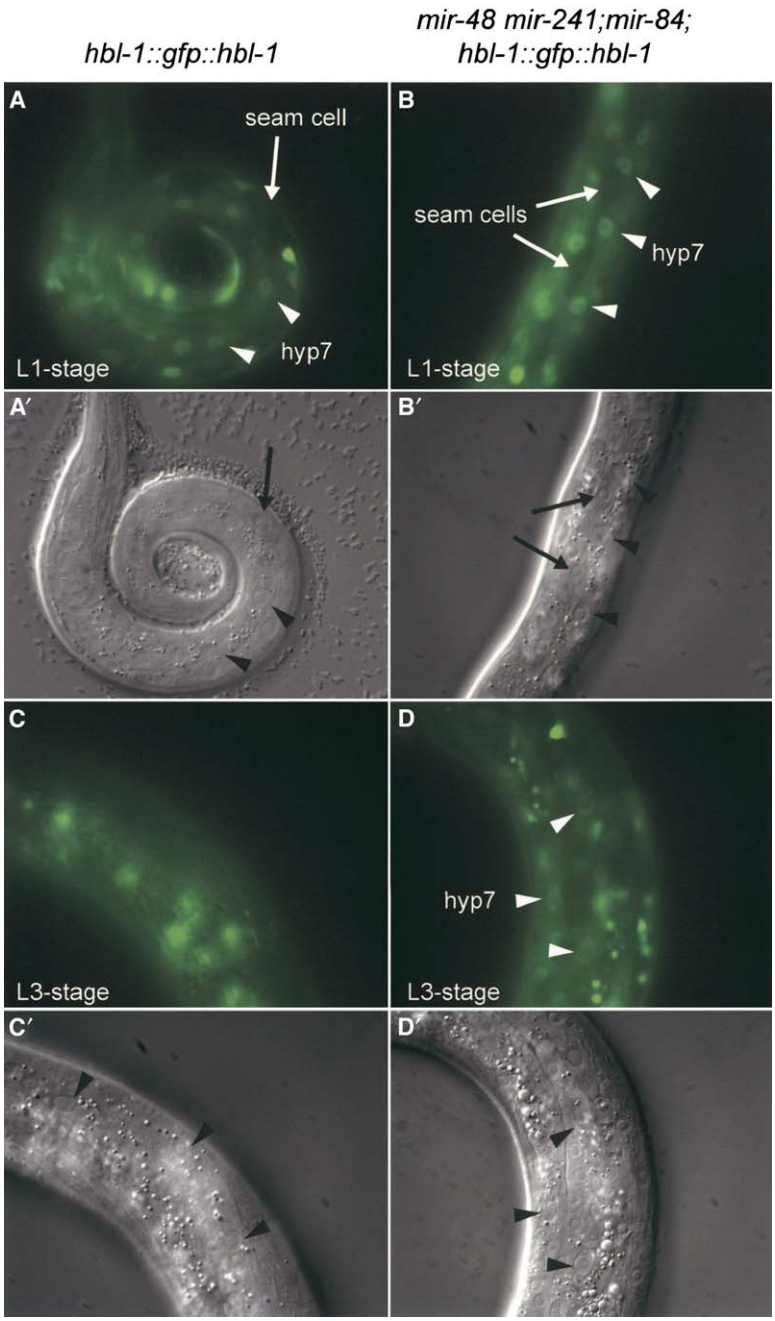

Figure 4. *mir-48*, *mir-84*, and *mir-241* Are Necessary for the Downregulation of *hbl-1::gfp::hbl-1* in the hyp7 Syncytium

(A–D) Larval stage and genotype are indicated for each panel. All fluorescent images were taken with identical exposure times. Fluorescent micrographs of a (A and C) wild-type and a (B and D) *mir-48 mir-241; mir-84* mutant animal carrying the *hbl-1::gfp::hbl-1* containing transgene *ctIs39* (Fay et al., 1999). (A and B) *hbl-1::gfp::hbl-1* is expressed at the L1 stage in hyp7 in a (A) wild-type and (B) *mir-48 mir-241; mir-84* mutant animal. Little or no expression is visible in the seam cells. Arrows indicate examples of seam cells, and arrowheads indicate examples of hyp7 nuclei. (C) *hbl-1::gfp::hbl-1* expression is undetectable in hyp7 in a L3-stage wild-type animal. (D) *hbl-1::gfp::hbl-1* expression is elevated in hyp7 in a L3-stage *mir-48 mir-241; mir-84* animal.

(A′–D′) Corresponding Nomarski DIC images for images shown in (A)–(D). Arrows indicate examples of seam cells, and arrowheads indicate examples of hyp7 nuclei.

animals, indicating that *hbl-1* functions downstream of the *let-7* family microRNAs. Moreover, the failure to appropriately downregulate *hbl-1* can be detected in the hypodermis of *mir-48 mir-241; mir-84* mutants and in neuronal cells of *let-7* mutants (Abrahante et al., 2003; Lin et al., 2003). The *hbl-1* 3′ UTR contains eight *let-7* complementary sites (Abrahante et al., 2003; Lin et al., 2003). Because these potential binding sites differ in sequence, each may be able to bind the individual *let-7* family microRNAs with differing efficacies. The relative contribution of individual *let-7* family microRNAs to the repression of *hbl-1* activity remains to be tested.

Previous studies showed a role for *hbl-1* activity in controlling the L4-to-adult transition (Abrahante et al., 2003; Lin et al., 2003). Our findings indicate that *hbl-1* also controls the L2-to-L3 transition in the hypodermis. This early role for *hbl-1* is consistent with the observation that reduction of *hbl-1* activity by RNAi results in a decreased number of seam cells in L2-stage animals (Abrahante et al., 2003). A reduced number of seam cells likely reflects a partial omission of the L2-stage proliferative program. This precocious phenotype is relatively weak in comparison to that of *lin-28*(lf) mutants, in which all seam cells generated from the V lineage fail to execute the L2-stage program (Ambros, 1989; Ambros and Horvitz, 1984; Moss et al., 1997). This weak

phenotype may be a consequence of residual *hbl-1* activity of the partial loss-of-function allele, *ve18*. It is possible that complete loss of *hbl-1* activity would result in a stronger precocious L2-omission phenotype similar to that seen in *lin-28*(lf) mutants.

mir-48, *mir-84*, and *mir-241* Function in Parallel to the *lin-28* and *lin-46* Pathway

An important regulator of the L2-to-L3 transition is *lin-28* (Ambros, 1989; Ambros and Horvitz, 1984; Moss et al., 1997), yet multiple lines of evidence suggest that the control of the L2-to-L3 transition by *mir-48*, *mir-84*, and *mir-241* does not occur through regulation of *lin-28* activity. First, a *lin-28::gfp::lin-28* reporter transgene that recapitulates the wild-type temporal regulation of LIN-28 protein and that rescues the phenotype of *lin-28*(lf) worms (Moss et al., 1997) was not derepressed in *mir-48 mir-241; mir-84* triple mutants. Second, we found that the level of endogenous LIN-28 protein was not significantly elevated in *mir-48 mir-241; mir-84* triple mutants, whereas, in *lin-4* retarded mutants, LIN-28 protein is abnormally abundant at later larval stages (Seggerson et al., 2002). Third, two alleles of *lin-58* that contain mutations upstream of *mir-48*, and hence lead to the misexpression of *mir-48*, enhance the precocious phenotype of a *lin-28* null mutant (Abrahante et al., 1998; Li et al., 2005), indicating that *mir-48* does not act exclusively through *lin-28*. Lastly, we found that the L2 reiteration phenotype of *mir-48 mir-241; mir-84* triple mutants could occur independently of *lin-28* activity. These data together indicate that *mir-48*, *mir-84*, and *mir-241* control the L2-to-L3 transition primarily through downstream effectors other than *lin-28*, even though the *lin-28* 3′ UTR contains a *let-7* complementary site. It is possible that the *let-7* family microRNAs may contribute to the repression of *lin-28* expression, but to a degree undetectable by our assays.

Our genetic epistasis analysis indicates that *mir-48*, *mir-84*, and *mir-241* function in parallel with the *lin-28* and *lin-46* pathway to downregulate *hbl-1* activity and hence control the L2-to-L3 transition (Table 1; Figure 5). One model to account for this convergence of pathways on *hbl-1* would be that LIN-46, in its putative role as a scaffolding protein (Pepper et al., 2004), could control assembly of a protein complex that directly interacts with HBL-1 protein to inhibit its activity in parallel with the repression of *hbl-1* mRNA translation exerted by *mir-48*, *mir-84*, and *mir-241*. Alternatively, LIN-46 could interact with RNA binding protein(s) and directly potentiate the activity of the *mir-48*, *mir-84*, and *mir-241* microRNAs.

mir-48, *mir-84*, and *mir-241* Coordinate Developmental Timing among Hypodermal Cell Types

Our data suggest that *mir-48*, *mir-84*, and *mir-241* control developmental timing in two physically associated but distinct cell types in the hypodermis: the postmitotic main body hypodermal syncytial cell, hyp7, and the proliferative seam cells. Two lines of evidence point to a role in hyp7 for *mir-48*, *mir-84*, and *mir-241* to repress *hbl-1* and control hyp7 temporal behavior. First, *mir-48; mir-84* mutant worms displayed heterochronic

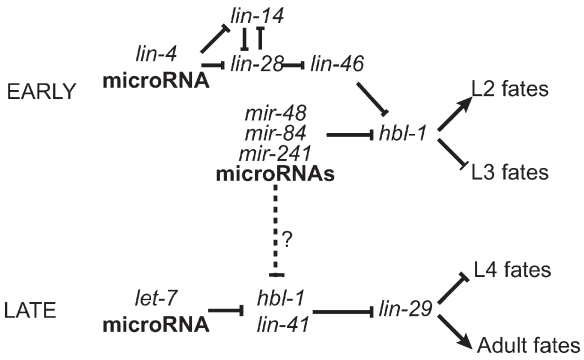

Figure 5. Model for the Early Role of *mir-48*, *mir-84*, and *mir-241* in the Heterochronic Gene Pathway at the L2-to-L3 Transition and the Late Role for *let-7* in the L4-to-Adult Transition

See text for details. Our data indicate that *mir-48*, *mir-84*, and *mir-241* act in parallel with *lin-28* and *lin-46* and upstream of *hbl-1* to control specification of L3-stage events. Both the *lin-28* and *lin-46* pathway and the *mir-48*, *mir-84*, *mir-241* pathway converge on *hbl-1* to specify the L2-to-L3 transition. *let-7* functions later to control specification of adult-stage events through its downstream effectors, *hbl-1* and *lin-41*. *mir-48*, *mir-84*, and *mir-241* control the exit from the molting cycle and may contribute to the repression of *hbl-1* and *lin-41* at the L4-to-adult transition.

defects in hyp7; the expression of the adult-specific transgene *col-19::gfp* was retarded in hyp7 but was regulated normally in the seam cells. Thus, the supernumerary molt observed in *mir-48; mir-84* double mutants may be a consequence of a heterochronic defect in hyp7. Second, our data indicate that *mir-48*, *mir-84*, and *mir-241* act in hyp7 to repress *hbl-1* activity. In *mir-48 mir-241; mir-84* worms, *hbl-1::gfp::hbl-1* was misregulated in hyp7. Thus, the 3′ UTR-dependent downregulation of *hbl-1::gfp::hbl-1* in hyp7 that occurs in wild-type animals (Abrahante et al., 2003; Lin et al., 2003) can be accounted for largely by the regulation of *hbl-1* by *mir-48*, *mir-84*, and *mir-241*.

mir-48, *mir-84*, and *mir-241* may also function in the hypodermal seam cells to control developmental timing. Reduction of *hbl-1* activity genetically or by *hbl-1* RNAi affected stage-specific behavior of seam cells, resulting in suppression of the retarded seam cell and alae phenotypes of *mir-48 mir-241; mir-84* worms. This could be a consequence of the repression of *hbl-1* by *mir-48*, *mir-84*, and *mir-241* in the seam cells. Interestingly, *hbl-1::gfp::hbl-1* cannot be detected in the seam cells after the L1 stage (Abrahante et al., 2003; Fay et al., 1999; Lin et al., 2003), suggesting that, at the time of the L2-to-L3 transition, the amount of *hbl-1* expression in seam cells is relatively low. Thus, *mir-48*, *mir-84*, and *mir-241* may function cell autonomously in the seam cells at the L3 stage to downregulate *hbl-1*, albeit beginning from a level already below the threshold of detection by our assays. Alternatively, since we could easily observe repression of *hbl-1::gfp::hbl-1* at the L2-to-L3 transition in hyp7, it is conceivable that the stage-specific behavior of seam cells may be controlled non-cell autonomously by a *hbl-1*-regulated signal from hyp7. Non-cell autonomous signaling from hyp7 to neighboring cells has been proposed in the pathway to

specify the fates of vulval precursor cells (VPCs). Mosaic analyses suggest that the sites of action of the multivulva (Muv) gene locus *lin-15* (Herman and Hedgecock, 1990) and of the synthetic Muv genes *lin-37* (Hedgecock and Herman, 1995) and *lin-35* (Myers and Greenwald, 2005) are in hyp7. One model is that hyp7 generates a signal to neighboring VPCs to inhibit vulval cell fate specification. Similarly, a signal from hyp7 to the lateral hypodermal seam cells may regulate the temporal behavior of seam cells and thereby help coordinate developmental timing throughout the hypodermis.

In summary, the results presented here demonstrate a role for the *let-7* family microRNA genes *mir-48*, *mir-84*, and *mir-241* in the heterochronic pathway to control the L2-to-L3 cell fate transitions in the hypodermis. Proper progression through the L1 and L2 larval stages requires downregulation of *lin-14* and *lin-28*, primarily through the action of the microRNA *lin-4*. Our findings extend the involvement of microRNAs in the regulation of *C. elegans* developmental timing to include a requirement for the downregulation of *hbl-1* by the combined action of the three *let-7* family microRNAs, *mir-48*, *mir-84*, and *mir-241* (Figure 5), in the hypodermis. We find that the L2-to-L3 transition is controlled by complex genetic mechanisms involving two microRNA-regulated pathways that converge on *hbl-1*: the *lin-4*, *lin-28*, *lin-46* pathway and the *mir-48*, *mir-84*, *mir-241* pathway (Figure 5). These parallel inputs to *hbl-1* may serve to couple *hbl-1* downregulation to distinct upstream temporal signals. Further, the functional redundancy among *mir-48*, *mir-84*, and *mir-241* could reflect alternative mechanisms for triggering the L2-to-L3 transition throughout the hypodermis. *mir-48*, *mir-84*, and *mir-241* seem to have more minor roles, compared to *let-7*, at the L4-to-adult transition in the hypodermis, indicating that different microRNA family members can be deployed for distinct roles, perhaps through differences in temporal or spatial expression patterns and/or differences in target specificity. These findings suggest that we may expect analogous forms of genetic redundancy and regulatory complexity in pathways involving other families of related microRNAs.

Experimental Procedures

Nematode Methods

C. elegans strains were grown under standard conditions as described (Wood et al., 1988). Strains used are listed in Table 1. The wild-type strain used was var. Bristol N2 (Brenner, 1974). Strains were grown at 20°C, except where otherwise indicated. For building multiply mutant strains, mutant alleles of *mir-48*, *mir-84*, and *mir-241* were identified by performing PCR reactions that amplified the genomic region flanking the deletion mutations. For the sequences of primers used to identify mutant alleles of *mir-48*, *mir-84*, and *mir-241*, see Table S1.

Identification, Isolation, and Rescue of MicroRNA Deletion Strains

Deletion mutants of *mir-48*, *mir-84*, and *mir-241* were isolated from a frozen library of EMS or UV-TMP mutagenized worms (Jansen et al., 1997; Liu et al., 1999). To enhance the detection of relatively small deletions, a "poison" primer was included in the first round of nested PCR reactions (Edgley et al., 2002). Additional detail is available in the Supplemental Data. For the sequences of primers used in identification of microRNA deletion strains, see Table S1.

Mutant alleles were backcrossed at least three times before further analysis. For rescue experiments, we injected pAAS50, a pCR-II TOPO plasmid containing a 5073 bp fragment that was amplified from genomic DNA from wild-type N2 worms. This fragment contains *mir-48* and *mir-241*, but no other experimentally defined or predicted gene. The sequences of the primers used to amplify the genomic DNA were 5′-CCAATTCTCTGTCTCCCCTTC-3′ and 5′-CAGAATTGTGTCGTCGTGTTC-3′. As a control, we used pAAS60, a plasmid generated from pAAS50 that lacked the sequences corresponding to the mature miR-48 and miR-241. The deletions were confirmed by sequence analysis of PCR-amplified genomic DNA sequences. To generate transgenic animals, germline transformation was performed as described (Mello and Fire, 1995). Plasmid DNA for pAAS50 or pAAS60 was injected (100 ng/μl) into *mir-48 mir-241(nDf51)* animals with pTG96 (*sur-5::gfp* at 20 ng/μl) as a coinjection marker. Seam cells were counted, alae were scored at the L4 molt, and worms were subsequently scored for GFP expression.

Northern Blot Analysis

Northern blots were performed as described (Lau et al., 2001; Lee and Ambros, 2001). Total RNA was isolated from a mixed population of animals for each strain, and 10 μg total RNA was loaded in each lane. To maximize the sensitivity of microRNA detection for developmental Northern blots, oligonucleotide probes were labeled with the Starfire Oligos Kit (IDT, Coralville, IA) and ^{32}P ATP (Amersham). Starfire oligonucleotide probes have approximately 10-fold greater specific activity as compared to traditional end-labeled oligonucleotide probes (Behlke et al., 2000). Probes used were the following ^{32}P end-labeled (Figure 1D) or Starfire-labeled (Figure 1B) oligonucleotides: 5′-TCGCATCTACTGAGCCTAC-3′ (miR-48), 5′-TACAATATTACATACTACC-3′ (miR-84), 5′-TCATTTCTCGCACCTACCT-3′ (miR-241), 5′-TCACACTTGAGGTCTCAGG-3′ (*lin-4* RNA), 5′-AACTATACAACCTACTACC-3′ (*let-7* RNA), and 5′-TGTCATCCTTGCGCAGG-3′ (U6 snRNA). For developmental Northern blots, RNA from staged animals was prepared as described in Lee and Ambros (2001). RNA samples were run on acrylamide denaturing gels and then transferred to GeneScreen Plus membranes (Perkin Elmer, Boston, MA) by electrophoresis. After transfer, blots were crosslinked with UV and baked at 80°C for 1 hr. Probes were hybridized to the membranes at 34°C in 7% SDS, 0.2 M Na_2PO_4 (pH 7.0) overnight. Membranes were washed at 34°C, twice with 2× SSPE, 0.1% SDS and twice with 0.5× SSPE, 0.1% SDS. The blots were exposed on Molecular Dynamics Phosphorimager screens, and signals were quantified by using ImageQuant (Molecular Dynamics).

Microscopy and Phenotype Analysis

The number of lateral hypodermal seam cells was counted at specific larval stages; staging was assessed by gonad morphology. Nomarski DIC microscopy was used to score seam cells and alae formation. Seam cells were identified according to their characteristic morphology and position along the lateral midline of the worm. Worms were anesthetized with 1 mM levamisole. Seam cells derived from the V lineage between the pharynx and the anus were scored on one side of individual animals. Cell lineage analysis was performed by picking individual L2-stage worms and monitoring seam cells derived from the V lineage as described by Sulston and Horvitz (1977), except that movies of worms were taken by using iVeZeen software (Boinx, Germering, Germany) and were analyzed with Quicktime software (Apple, Cupertino, CA). Three *mir-48 mir-241* and three *mir-48 mir-241; mir-84* animals were analyzed. Electron microscopy of adult animals was performed as described (Bargmann et al., 1993).

RNAi Assays

The plasmid pAA26, which expresses *hbl-1* dsRNA, was constructed by amplifying a 1.5 kb region from genomic DNA, digesting with NotI, and inserting into the NotI site of the cloning vector pPD129.36 (Timmons et al., 2001) with convergent T7 promoters. Oligonucleotides used for *hbl-1* amplification were AA141, 5′-ATCTATGCGGCCGCGACGGTGCTCAATCAGATAGC-3′, and AA142, 5′-ATCTATGCGGCCGCGACGGTGCTCAATCAGATAGC-3′. pAA26 was

transformed into bacterial strain HT115 (Timmons et al., 2001). RNAi of *lin-41* was performed by using a bacterial strain obtained from the MRC geneservice (Cambridge, UK), gene pair name C12C8.3 (Fraser et al., 2000; Kamath and Ahringer, 2003). dsRNA-expressing bacteria were grown from single colonies overnight in LB with 200 μg/ml ampicillin and 12.5 μg/ml tetracycline and were then plated on NGM plates containing 1 mM IPTG, 200 μg/ml ampicillin, and 12.5 μg/ml tetracycline. For suppression of *hbl-1* and *lin-41*, overnight cultures of each bacterial strain were mixed 1:1 and plated. Embryos were hatched on plates with dsRNA-expressing bacteria, and larvae were scored by using Nomarski DIC microscopy at indicated stages for seam cell and alae phenotypes.

Supplemental Data

Supplemental Data including Supplemental Experimental Procedures, a figure, and a table are available at http://www.developmentalcell.com/cgi/content/full/9/3/403/DC1/.

Acknowledgments

We thank Rosalind Lee and Chris Hammell for RNA preparation and Northern blot analysis, Andrew Hellman for performing PCR screening for deletion mutations, Beth Castor for DNA sequence determinations, Na An for strain management, Erika Hartwieg for performing EM analyses, and the *Caenorhabditis* Genetics Center for strains. The *Caenorhabditis* Genetics Center is supported by the National Institutes of Health (NIH) National Center for Research Resources. A.L.A. was supported by a Ruth L. Kirschstein National Research Service Award postdoctoral fellowship (5F32GM065721-02). E.A.M. was a Wellcome Trust Prize Traveling Research Fellow (#061641). D.P.B. and V.A. were supported by grants from the NIH (GM067031 to D.P.B and GM34028 to V.A.). H.R.H. is the David H. Koch Professor of Biology at Massachusetts Institute of Technology and was supported by and is an Investigator of the Howard Hughes Medical Institute.

Received: May 9, 2005
Revised: July 26, 2005
Accepted: July 27, 2005
Published: September 6, 2005

References

Abrahante, J.E., Miller, E.A., and Rougvie, A.E. (1998). Identification of heterochronic mutants in *Caenorhabditis elegans*. Temporal misexpression of a collagen:green fluorescent protein fusion gene. Genetics *149*, 1335–1351.

Abrahante, J.E., Daul, A.L., Li, M., Volk, M.L., Tennessen, J.M., Miller, E.A., and Rougvie, A.E. (2003). The *Caenorhabditis elegans hunchback*-like gene *lin-57/hbl-1* controls developmental time and is regulated by microRNAs. Dev. Cell *4*, 625–637.

Ambros, V. (1989). A hierarchy of regulatory genes controls a larva-to-adult developmental switch in *C. elegans*. Cell *57*, 49–57.

Ambros, V., and Horvitz, H.R. (1984). Heterochronic mutants of the nematode *Caenorhabditis elegans*. Science *226*, 409–416.

Ambros, V., Lee, R.C., Lavanway, A., Williams, P.T., and Jewell, D. (2003). MicroRNAs and other tiny endogenous RNAs in *C. elegans*. Curr. Biol. *13*, 807–818.

Bargmann, C.I., Hartwieg, E., and Horvitz, H.R. (1993). Odorant-selective genes and neurons mediate olfaction in *C. elegans*. Cell *74*, 515–527.

Bartel, D.P. (2004). MicroRNAs: genomics, biogenesis, mechanism, and function. Cell *116*, 281–297.

Behlke, M.A., Dames, S.A., McDonald, W.H., Gould, K.L., Devor, E.J., and Walder, J.A. (2000). Use of high specific activity StarFire oligonucleotide probes to visualize low-abundance pre-mRNA splicing intermediates in *S. pombe*. Biotechniques *29*, 892–897.

Beitel, G.J., Clark, S.G., and Horvitz, H.R. (1990). *Caenorhabditis elegans ras* gene *let-60* acts as a switch in the pathway of vulval induction. Nature *348*, 503–509.

Berezikov, E., Guryev, V., van de Belt, J., Wienholds, E., Plasterk, R.H., and Cuppen, E. (2005). Phylogenetic shadowing and computational identification of human microRNA genes. Cell *120*, 21–24.

Brennecke, J., Stark, A., Russell, R.B., and Cohen, S.M. (2005). Principles of microRNA-target recognition. PLoS Biol. *3*, e85.

Brenner, S. (1974). The genetics of *Caenorhabditis elegans*. Genetics *77*, 71–94.

Doench, J.G., and Sharp, P.A. (2004). Specificity of microRNA target selection in translational repression. Genes Dev. *18*, 504–511.

Edgley, M., D'Souza, A., Moulder, G., McKay, S., Shen, B., Gilchrist, E., Moerman, D., and Barstead, R. (2002). Improved detection of small deletions in complex pools of DNA. Nucleic Acids Res. *30*, e52.

Fay, D.S., Stanley, H.M., Han, M., and Wood, W.B. (1999). A *Caenorhabditis elegans* homologue of *hunchback* is required for late stages of development but not early embryonic patterning. Dev. Biol. *205*, 240–253.

Fraser, A.G., Kamath, R.S., Zipperlen, P., Martinez-Campos, M., Sohrmann, M., and Ahringer, J. (2000). Functional genomic analysis of *C. elegans* chromosome I by systematic RNA interference. Nature *408*, 325–330.

Grad, Y., Aach, J., Hayes, G.D., Reinhart, B.J., Church, G.M., Ruvkun, G., and Kim, J. (2003). Computational and experimental identification of *C. elegans* microRNAs. Mol. Cell *11*, 1253–1263.

Grosshans, H., Johnson, T., Reinert, K.L., Gerstein, M., and Slack, F.J. (2005). The temporal patterning microRNA *let-7* regulates several transcription factors at the larval to adult transition in *C. elegans*. Dev. Cell *8*, 321–330.

Han, M., and Sternberg, P.W. (1990). *let-60*, a gene that specifies cell fates during *C. elegans* vulval induction, encodes a *ras* protein. Cell *63*, 921–931.

Hedgecock, E.M., and Herman, R.K. (1995). The *ncl-1* gene and genetic mosaics of *Caenorhabditis elegans*. Genetics *141*, 989–1006.

Herman, R.K., and Hedgecock, E.M. (1990). Limitation of the size of the vulval primordium of *Caenorhabditis elegans* by *lin-15* expression in surrounding hypodermis. Nature *348*, 169–171.

Jansen, G., Hazendonk, E., Thijssen, K.L., and Plasterk, R.H. (1997). Reverse genetics by chemical mutagenesis in *Caenorhabditis elegans*. Nat. Genet. *17*, 119–121.

Johnson, S.M., Grosshans, H., Shingara, J., Byrom, M., Jarvis, R., Cheng, A., Labourier, E., Reinert, K.L., Brown, D., and Slack, F.J. (2005). *RAS* is regulated by the *let-7* microRNA family. Cell *120*, 635–647.

Kamath, R.S., and Ahringer, J. (2003). Genome-wide RNAi screening in *Caenorhabditis elegans*. Methods *30*, 313–321.

Kloosterman, W.P., Wienholds, E., Ketting, R.F., and Plasterk, R.H. (2004). Substrate requirements for *let-7* function in the developing zebrafish embryo. Nucleic Acids Res. *32*, 6284–6291.

Lai, E.C. (2002). Micro RNAs are complementary to 3′ UTR sequence motifs that mediate negative post-transcriptional regulation. Nat. Genet. *30*, 363–364.

Lau, N.C., Lim, L.P., Weinstein, E.G., and Bartel, D.P. (2001). An abundant class of tiny RNAs with probable regulatory roles in *Caenorhabditis elegans*. Science *294*, 858–862.

Lee, R.C., and Ambros, V. (2001). An extensive class of small RNAs in *Caenorhabditis elegans*. Science *294*, 862–864.

Lee, R.C., Feinbaum, R.L., and Ambros, V. (1993). The *C. elegans* heterochronic gene *lin-4* encodes small RNAs with antisense complementarity to *lin-14*. Cell *75*, 843–854.

Lewis, B.P., Shih, I.H., Jones-Rhoades, M.W., Bartel, D.P., and Burge, C.B. (2003). Prediction of mammalian microRNA targets. Cell *115*, 787–798.

Lewis, B.P., Burge, C.B., and Bartel, D.P. (2005). Conserved seed pairing, often flanked by adenosines, indicates that thousands of human genes are microRNA targets. Cell *120*, 15–20.

Li, M., Jones-Rhoades, M.W., Lau, N.C., Bartel, D.P., and Rougvie, A.E. (2005). Regulatory mutations of *mir-48*, a *C. elegans let-7* fam-

ily microRNA, cause developmental timing defects. Dev. Cell *9*, this issue, 415–422.

Lim, L.P., Lau, N.C., Weinstein, E.G., Abdelhakim, A., Yekta, S., Rhoades, M.W., Burge, C.B., and Bartel, D.P. (2003). The microRNAs of *Caenorhabditis elegans*. Genes Dev. *17*, 991–1008.

Lim, L.P., Lau, N.C., Garrett-Engele, P., Grimson, A., Schelter, J.M., Castle, J., Bartel, D.P., Linsley, P.S., and Johnson, J.M. (2005). Microarray analysis shows that some microRNAs downregulate large numbers of target mRNAs. Nature *433*, 769–773.

Lin, S.Y., Johnson, S.M., Abraham, M., Vella, M.C., Pasquinelli, A., Gamberi, C., Gottlieb, E., and Slack, F.J. (2003). The *C. elegans hunchback* homolog, *hbl-1*, controls temporal patterning and is a probable microRNA target. Dev. Cell *4*, 639–650.

Liu, L.X., Spoerke, J.M., Mulligan, E.L., Chen, J., Reardon, B., Westlund, B., Sun, L., Abel, K., Armstrong, B., Hardiman, G., et al. (1999). High-throughput isolation of *Caenorhabditis elegans* deletion mutants. Genome Res. *9*, 859–867.

Liu, Z., Kirch, S., and Ambros, V. (1995). The *Caenorhabditis elegans* heterochronic gene pathway controls stage-specific transcription of collagen genes. Development *121*, 2471–2478.

Mallory, A.C., Reinhart, B.J., Jones-Rhoades, M.W., Tang, G., Zamore, P.D., Barton, M.K., and Bartel, D.P. (2004). MicroRNA control of PHABULOSA in leaf development: importance of pairing to the microRNA 5′ region. EMBO J. *23*, 3356–3364.

Mello, C.C., and Fire, A. (1995). DNA transformation. In Methods in Cell Biology: *Caenorhabditis elegans*: Modern Biological Analysis of an Organism, H.F. Epstein and D.C. Shakes, eds. (San Diego, CA: Academic Press), pp. 451–482.

Moss, E.G., Lee, R.C., and Ambros, V. (1997). The cold shock domain protein LIN-28 controls developmental timing in *C. elegans* and is regulated by the *lin-4* RNA. Cell *88*, 637–646.

Myers, T.R., and Greenwald, I. (2005). *lin-35* Rb Acts in the major hypodermis to oppose *Ras*-mediated vulval induction in *C. elegans*. Dev. Cell *8*, 117–123.

Ohler, U., Yekta, S., Lim, L.P., Bartel, D.P., and Burge, C.B. (2004). Patterns of flanking sequence conservation and a characteristic upstream motif for microRNA gene identification. RNA *10*, 1309–1322.

Pasquinelli, A.E., Reinhart, B.J., Slack, F., Martindale, M.Q., Kuroda, M.I., Maller, B., Hayward, D.C., Ball, E.E., Degnan, B., Muller, P., et al. (2000). Conservation of the sequence and temporal expression of *let-7* heterochronic regulatory RNA. Nature *408*, 86–89.

Pepper, A.S., McCane, J.E., Kemper, K., Yeung, D.A., Lee, R.C., Ambros, V., and Moss, E.G. (2004). The *C. elegans* heterochronic gene *lin-46* affects developmental timing at two larval stages and encodes a relative of the scaffolding protein gephyrin. Development *131*, 2049–2059.

Reinhart, B.J., Slack, F.J., Basson, M., Pasquinelli, A.E., Bettinger, J.C., Rougvie, A.E., Horvitz, H.R., and Ruvkun, G. (2000). The 21-nucleotide *let-7* RNA regulates developmental timing in *Caenorhabditis elegans*. Nature *403*, 901–906.

Rougvie, A.E. (2001). Control of developmental timing in animals. Nat. Rev. Genet. *2*, 690–701.

Seggerson, K., Tang, L., and Moss, E.G. (2002). Two genetic circuits repress the *Caenorhabditis elegans* heterochronic gene *lin-28* after translation initiation. Dev. Biol. *243*, 215–225.

Slack, F.J., Basson, M., Liu, Z., Ambros, V., Horvitz, H.R., and Ruvkun, G. (2000). The *lin-41* RBCC gene acts in the *C. elegans* heterochronic pathway between the *let-7* regulatory RNA and the LIN-29 transcription factor. Mol. Cell *5*, 659–669.

Stark, A., Brennecke, J., Russell, R.B., and Cohen, S.M. (2003). Identification of *Drosophila* MicroRNA targets. PLoS Biol. *1*, E60.

Sulston, J.E., and Horvitz, H.R. (1977). Post-embryonic cell lineages of the nematode, *Caenorhabditis elegans*. Dev. Biol. *56*, 110–156.

Timmons, L., Court, D.L., and Fire, A. (2001). Ingestion of bacterially expressed dsRNAs can produce specific and potent genetic interference in *Caenorhabditis elegans*. Gene *263*, 103–112.

Vella, M.C., Choi, E.Y., Lin, S.Y., Reinert, K., and Slack, F.J. (2004). The *C. elegans* microRNA *let-7* binds to imperfect *let-7* complementary sites from the *lin-41* 3′UTR. Genes Dev. *18*, 132–137.

Wightman, B., Ha, I., and Ruvkun, G. (1993). Posttranscriptional regulation of the heterochronic gene *lin-14* by *lin-4* mediates temporal pattern formation in *C. elegans*. Cell *75*, 855–862.

Wood, W.B., and the Community of *C. elegans* Researchers (1988). The Nematode *Caenorhabditis elegans* (Cold Spring Harbor, NY: Cold Spring Harbor Laboratory Press).